

Supporting Information

Influence of horizontal centrifugation processes on the content of phenolic secoiridoids and their oxidized derivatives in commercial olive oils: an insight by liquid chromatography – high resolution mass spectrometry and chemometrics

C. De Ceglie^a, R. Abbattista^a, I. Losito^{a,b*}, A. Castellaneta^a, C.D. Calvano^{b,c}, G. Bianco^d, F. Palmisano^{a,b}, T.R.I. Cataldi^{a,b}

^aDipartimento di Chimica, ^bCentro Interdipartimentale SMART and ^cDipartimento di Farmacia e Scienze del Farmaco, Università degli Studi di Bari “Aldo Moro”, via Orabona 4, 70126 Bari (Italy)

^dDipartimento di Scienze, Università degli Studi della Basilicata, via dell’Ateneo Lucano, 10-85100, Potenza (Italy)

Supporting Information content:

Table S1. Summary of the production-related information provided by producers on the 22 olive oils analysed during the study.

Table S2. Summary of means and standard deviations obtained for each of the seven secoiridoids under study from normalized XIC peak areas referred to two- and three-phase olive oils.

Figure S1. Schematic representation of the complex ensemble of enzymatic (indicated by thick white arrows) and chemical processes proposed to explain the generation of the different isoforms found in olive oils for oleuropein and ligstroside aglycones (OA/LA) and for oleacin and oleocanthal. The numbers used to label different chromatographic peaks referred to OA and LA isoforms (see Figure 1 in the main text) are the same adopted in Refs. 31 and 32 cited in the main text. Note that chiral centres are labelled with an asterisk; wavy bonds indicate that both possible configurations at chiral centres or both geometries on C=C bonds, according to the case, are possible.

Figure S2. Schematic representation of MS/MS fragmentations leading to isoforms of oxidized decarboxymethyl-elenolic acid, i.e. decarboxymethyl-elenolic acid with an aldehydic moiety oxidized to a carboxylic one. The depicted processes were exploited to recognize peaks related to the possible isoforms of oleocanthal carboxylate in the XIC traces referred to oleacin obtained after the RPC-ESI(-)-FTMS analyses of olive oil extracts. Note that the negative charge of product ions is shown only for one of both possible ionization sites, i.e. the two COOH groups, when two of these are present. For the sake of simplicity, only the oxidized forms of *Open Forms I* and *Closed Forms I* of oleocanthal are shown as precursors, yet the oxidation to carboxylic acid could occur also on one of the C=O groups of oleocanthal *Open Forms II* (see Figure S1 for their structures).

Figure S3. Schematic representation of MS/MS fragmentations leading to isoforms of oxidized elenolic acid, i.e., elenolic acid with an aldehydic moiety oxidized to a carboxylic one, which were exploited to recognize peaks related to the possible isoforms of ligstroside aglycone oxidized to carboxylic acid in the XIC traces referred to oleuropein aglycone obtained after the RPC-ESI(-)-FTMS analyses of olive oil extracts. Note that the negative charge of product ions is shown only for one of the two possible ionization sites, the two COOH groups, when two of these are present. For the sake of simplicity, only the oxidized forms of *Open Forms I*, *Closed Forms I* and one of those potentially related to *Closed Forms II* of ligstroside aglycone are shown as precursors. In principle, oxidation to carboxylic acid could occur also on one of the C=O groups of *Open Forms II* and on the other C=O group of *Closed Forms II* (see Figure S1 for their structures).

Table S1. Summary of production-related information provided by producers on the 22 olive oils analysed during the study.

Oil #	Olive cultivar(s)	Year of production	Type of horizontal centrifugation	Type of crushing	Malaxation temperature/time (min)	Additional features ^a
1	<i>Coratina</i>	2017	Three-phase	Stone mill	26°C / 30 min	
2	<i>Coratina</i>	2017	Three-phase	Stone mill	26°C / 30 min	
3	<i>Coratina</i>	2017	Three-phase	Stone mill	26°C / 30 min	
4	<i>Coratina</i>	2018	Three-phase	Crusher	27°C / 40 min	
5	<i>Coratina</i>	2018	Three-phase	Crusher	27°C / 30 min	
6	<i>Coratina</i>	2018	Three-phase	Crusher	27°C / 30 min	
7	<i>Coratina</i>	2018	Three-phase	Crusher	26°C / 40 min	
8	<i>Coratina</i>	2018	Three-phase	Crusher	23°C / 30 min	
9	<i>Coratina</i>	2018	Three-phase	Crusher	23°C / 30 min	
10	<i>Coratina</i>	2018	Three-phase	Crusher	26°C / 30 min	1) Olives harvested in Southern Apulia (Taranto) ^b 2) Blade crusher 3) No vertical centrifugation 4) Inert atmosphere (nitrogen) during storage
11	<i>Peranzana</i>	2018	Three-phase	Crusher	29°C / 30 min	
12	<i>Peranzana</i>	2018	Three-phase	Crusher	29°C / 30 min	
13	<i>Leccino/Coratina</i>	2018	Three-phase	Stone mill	23°C / 40 min	Olives harvested in Southern Apulia (Brindisi) ^b
14	<i>Coratina</i>	2018	Three-phase	Crusher	27°C / 90 s Pieralisi Protoreactor®	Olive grove affected by <i>B. olea</i> (olive fruit fly)
15	<i>Coratina</i>	2017	Two-phase	Crusher	26°C / 30 min	
16	<i>Coratina</i>	2018	Two-phase	Crusher	26°C / 30 min	
17	<i>Coratina</i>	2018	Two-phase	Crusher	23°C / 10 min	1) De-stoned olives used 2) Production under inert atmosphere (nitrogen)

18	<i>Coratina</i>	2018	Two-phase	Crusher	23 °C / 10 min	Production under inert atmosphere (nitrogen)
19	<i>Coratina</i>	2018	Two-phase	Crusher	26°C / 30 min	
20	<i>Coratina/Ogliarola</i>	2018	Two-phase	Crusher	27°C / 40 min	
21	<i>Coratina</i>	2018	Two-phase	Crusher	23°C / 20 min	
22	<i>Coratina</i>	2018	Two-phase	Crusher	21°C / 12 min	1) Blade crusher 2) Inert atmosphere (nitrogen) during malaxation and storage 3) No vertical centrifugation

^aUnless specified differently among additional features, all olive oils were obtained using vertical centrifugation as the last step of the productive process and hammer crushers were used when a mechanical crusher was adopted in the first step of production.

^{*}Oils labelled as #10 and #13 were the only ones, among those produced in 2018, that were obtained from olives harvested in Southern Apulia (Taranto and Brindisi provinces). This area was not interested by snowfalls and frosts that occurred in early spring 2018 (with negative consequences on the olive oil production during the 2018/2019 campaign) in Northern Apulia (Bari and Bisceglie-Andria-Trani provinces), where all the other oils were produced.

Table S2. Summary of means and standard deviations obtained for each of the seven secoiridoids under study from normalized XIC peak areas referred to olive oils produced using two- or three-phase decanters for horizontal centrifugation.

Secoiridoid	Mean values \pm standard deviations		Difference between means*
	Two-phase	Three-phase	
Oleuropein aglycone	4.3 ± 1.5	1.7 ± 0.8	Significant (p = 0.0000)
Ligstroside aglycone	2.9 ± 1.7	1.4 ± 0.9	Significant (p = 0.0129)
Oleacin	1.4 ± 0.7	0.8 ± 0.4	Significant (p = 0.0179)
Oleocanthal	0.8 ± 0.3	0.7 ± 0.3	Not significant (p = 0.4608)
Oleuropein aglycone carboxylic acid	0.10 ± 0.07	0.05 ± 0.02	Significant (p = 0.0196)
Oleacin carboxylic acid	0.04 ± 0.03	0.03 ± 0.03	Not significant (p = 0.4608)
Oleocanthal carboxylic acid	0.08 ± 0.09	0.04 ± 0.07	Not significant (p = 0.2584)

*The statistical significance of differences between mean was evaluated using a Tukey-Kramer test at 95% confidence.

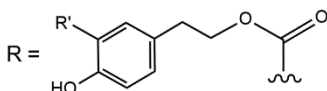


Figure S1. Schematic representation of the complex ensemble of enzymatic (indicated by thick white arrows) and chemical processes proposed to explain the generation of the different isoforms found in olive oils for oleuropein and ligstroside aglycones (OA/LA) and for oleacin and oleocanthal. The numbers used to label different chromatographic peaks referred to OA and LA isoforms (see Figure 1 in the main text) are the same adopted in Refs. 31 and 32 cited in the main text. Note that chiral centres are labelled with an asterisk; wavy bonds indicate that both possible configurations at chiral centres or both geometries on C=C bonds, according to the case, are possible.

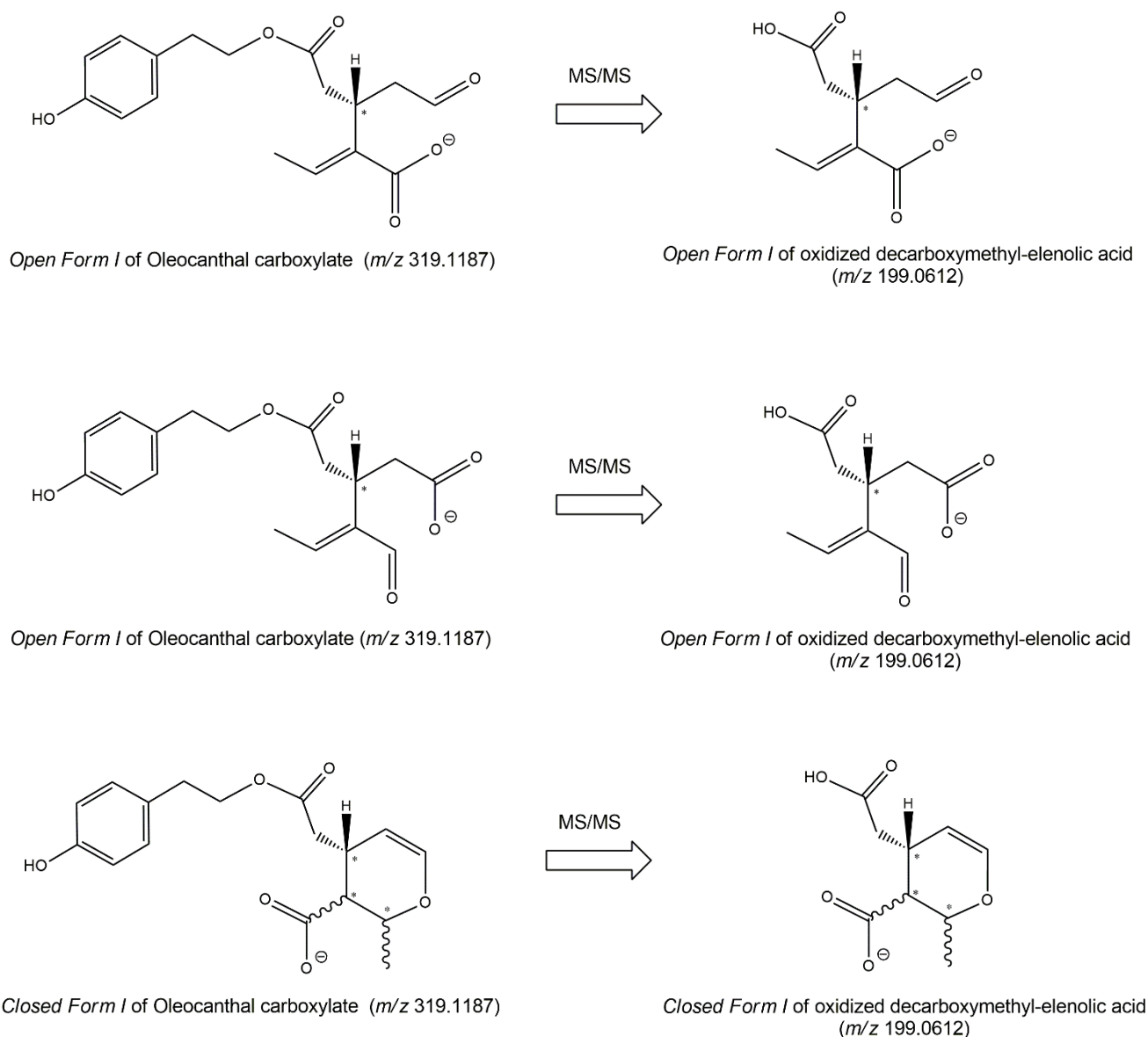


Figure S2. Schematic representation of MS/MS fragmentations leading to isoforms of oxidized decarboxymethyl-elenolic acid, i.e. decarboxymethyl-elenolic acid with an aldehydic moiety oxidized to a carboxylic one. The depicted processes were exploited to recognize peaks related to the possible isoforms of oleocanthal carboxylate in the XIC traces referred to oleacin obtained after the RPC-ESI(-)-FTMS analyses of olive oil extracts. Note that the negative charge of product ions is shown only for one of both possible ionization sites, i.e. the two COOH groups, when two of these are present. For the sake of simplicity, only the oxidized forms of *Open Forms I* and *Closed Forms I* of oleocanthal are shown as precursors, yet the oxidation to carboxylic acid could occur also on one of the C=O groups of oleocanthal *Open Forms II* (see Figure S1 for their structures).

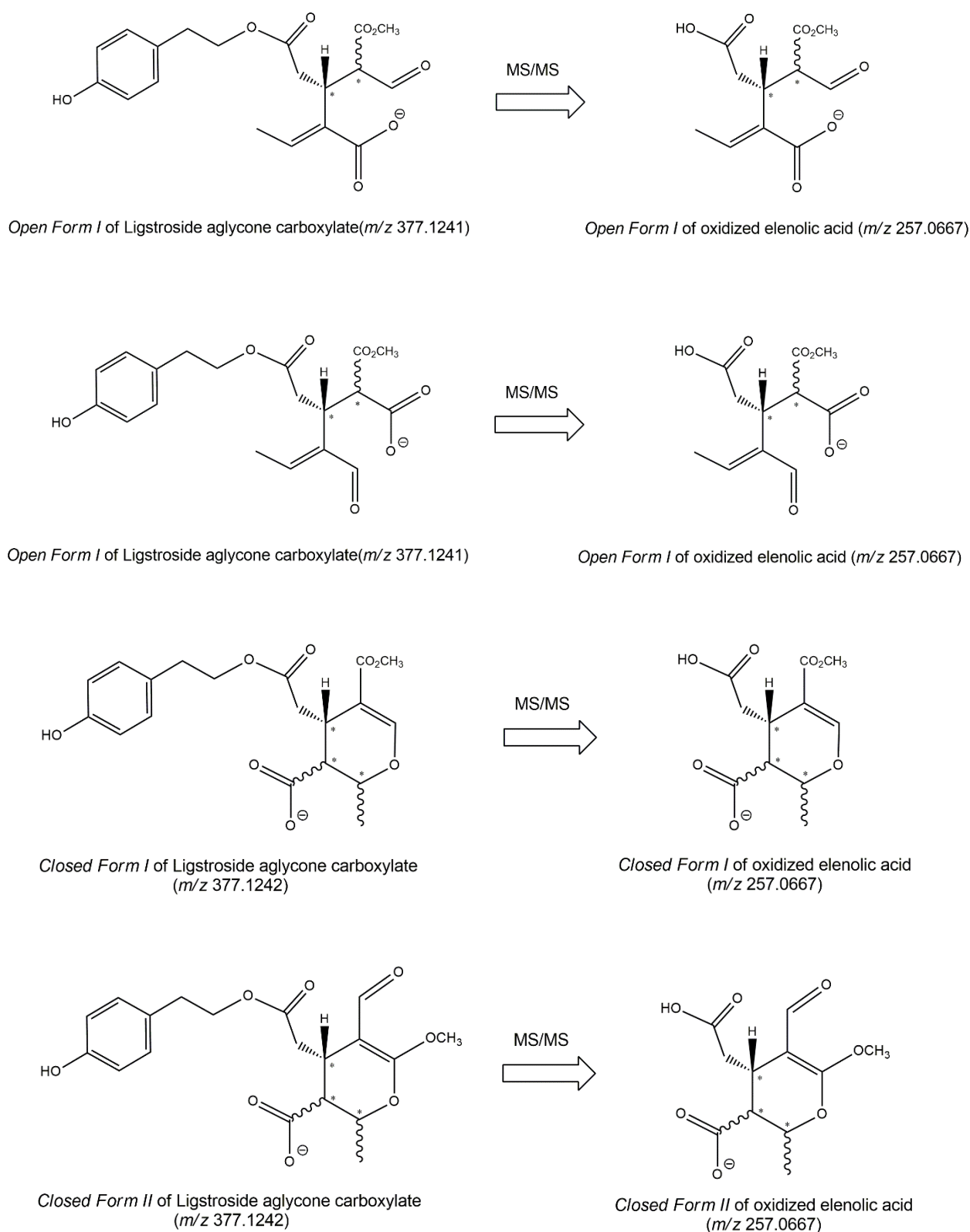


Figure S3. Schematic representation of MS/MS fragmentations leading to isoforms of oxidized elenolic acid, i.e., elenolic acid with an aldehydic moiety oxidized to a carboxylic one, which were exploited to recognize peaks related to the possible isoforms of ligstroside aglycone oxidized to carboxylic acid in the XIC traces referred to oleuropein aglycone obtained after the RPC-ESI(-)-FTMS analyses of olive oil extracts. Note that the negative charge of product ions is shown only for one of the two possible ionization sites, the two COOH groups, when two of these are present. For the sake of simplicity, only the oxidized forms of *Open Forms I*, *Closed Forms I* and one of those potentially related to *Closed Forms II* of ligstroside aglycone are shown as precursors. In principle, oxidation to carboxylic acid could occur also on one of the C=O groups of *Open Forms II* and on the other C=O group of *Closed Forms II* (see Figure S1 for their structures).